Mars Landing Vehicles: Descent and Ascent Propulsion Design Issues

Bryan Palaszewski
Engine Combustion Branch
NASA Glenn Research Center
MS 5-10
21000 Brookpark Road
Cleveland, OH 44135
bryan.a.palaszewski@nasa.gov

Abstract

Human and robotic Mars missions often include plans for landing large payloads on the planet's surface. Thus far, landing of payload of up to approximately 1 metric ton (MT) have been successful. Future human missions have suggested large 5 to 25 MT surface payloads may be needed. Therefore, large landing vehicles with an initial mass of up to 100 MT may be required. In this chapter, the future human payload missions are assessed, investigating the mission velocity changes (delta-V) values for deorbit, deceleration, landing and ascent. The initial masses of single and multi-stage Mars landing vehicles are computed. Issues related to vehicle mass factors and delivering the needed delta-V are discussed.

Keywords: Mars, landing, chemical propulsion, descent, deorbit, deceleration, hover, ascent, in-situ resource utilization, orbital transfer

1.0 Introduction

Current Mars missions use robotic vehicles, including flyby spacecraft, orbiters, landers, rovers, and an experimental helicopter. The first Mars flyby, Mariner 4, was launched in 1964 and returned the first close up photographs of its surface. Additional Mars flybys were conducted in 1969: Mariners 6 and 7. The Mariner 9 spacecraft successfully entered Mars orbit in 1973. Using its photographs, the Mars Viking Orbiters and Landers 1 and 2 were launched in 1975 and successfully landed in 1976. Life detection experiments were part of the landers' payload. While those experiments were negative or at best inconclusive, many Mars missions were planned for more ambitious robotic and human missions.

The Mars 2020 Perseverance Mission is the most recent Mars rover. The rover mass is approximately 1 metric ton (MT). The rovers on Mars have made crucial measurements of the nature of the rock and regolith; the surface measurement will improve our understanding of potential chemical compatibility of humans and machines with the surface for future Mars base camps and colonies. Preceding the Mars 2020 rover were the Mars Pathfinder rover in 1997, the two Mars Exploration Rovers (MER) in 2004 and the Mars Science Laboratory (MSL) rover in 2012.

In the 1960's after the Mariner 4 flyby mission's atmospheric radio transmission experiments, Mars landing studies focused on using the very thin martian atmosphere for landing. The atmospheric density is only approximately 1/100th that of Earth's atmospheric density. Landing in such a thin atmosphere will require rocket propulsion. For smaller robotic landers, a combination of parachutes and rocket engines for landing was successfully used on the Viking Landers. The 1997 Mars Pathfinder mission used parachutes and rocket engines and an additional inflatable airbag system for a bouncing and rolling landing.

Human Mars missions have been planned and analyzed since the 1950's and continue to this day. The most recent Mars architectures' primary interplanetary transportation vehicles (ITV) include chemical propulsion, nuclear thermal propulsion, and nuclear electric propulsion. Landing vehicles have been included for either the martian moons or Mars surface exploration. In all case, chemical propulsion is nominally used for the Mars ascent-descent vehicles or landers.

Human mission design has evolved over many years, but always required rocket propulsion. Lander studies have investigated low, medium, and high lift to drag (L/D) aerodynamic designs. Figure 1 depicts a low L/D lander (Ref. 1, Woodcock). This lander is a 2 stage design, and the overall entry shape is like the Apollo command module. Figure 2 presents a mid L/D entry lander (Ref. 2); it was designed to deliver an ascent vehicle encapsulated in the aerodynamic shell. Typically, the low L/D lander designs have been the focus of the most recent lander architectures: the NASA 90 Day Study (1989, 1990), Boeing Space Transfer Concepts, Mars Design Reference Mission 5 (2002), The Mars Base Camp (2017) (Refs. 3, 4, 5 6 and 7).

2.0 Mission design and delta-V

There are several important Mars lander mission delta-V elements. They include Deorbit, Deceleration, Hover, and Ascent. Each of these delta-V values reflects the major maneuvers for the lander. References 8 and 9 provided the details of many of the orbital mechanics analyses.

2.1 Deorbit

Once the human Mars interplanetary transportation vehicle (ITV) enters Mars orbit, the lander is designed to descend from Mars orbit. The main Mars transportation system may be in in either an elliptical or circular orbit. An initial elliptical orbit is often used to reduce the delta-V to enter Mars orbit. A circular orbit is often selected after the Mars interplanetary transportation vehicle (ITV) to reduce the delta-V for the Mars lander. Thus, there is often a balance between the ITVs orbit and the total mass of the lander and the ITV.

An option of the lander entering orbit from the interplanetary trajectory apart from the main Mars transportation vehicle has been considered. This option was used in the Refs. 3, 4, and 5 studies. An aerobrake was used for the lander's entry into orbit and for the final Mars descent and landing.

The deorbit delta-V is shown in Figure 3.

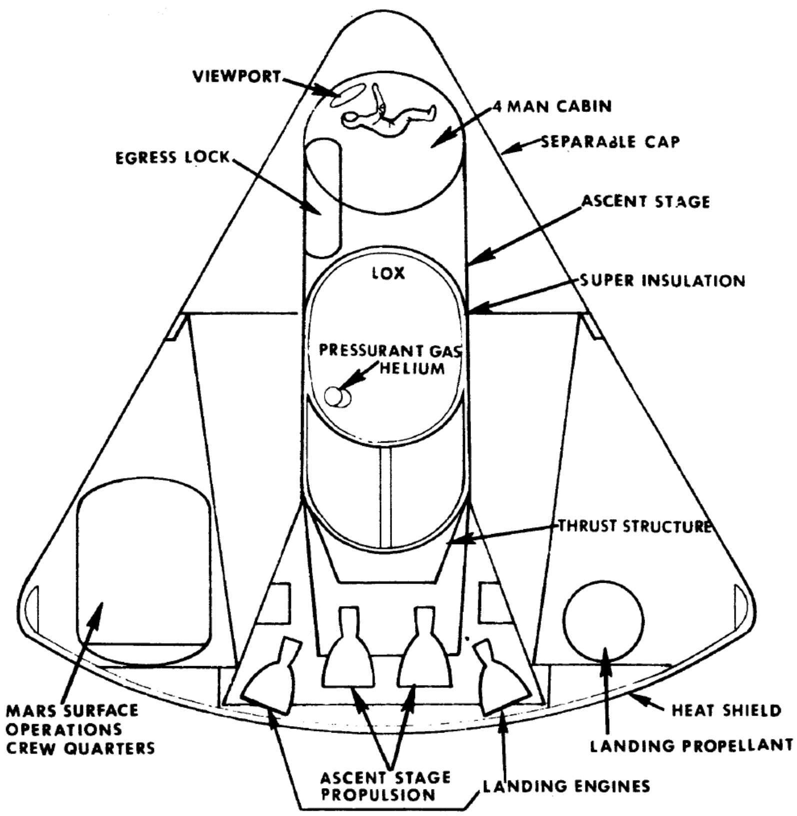

Figure 1. Mars Excursion Module (MEM) lander design (ref. 1)

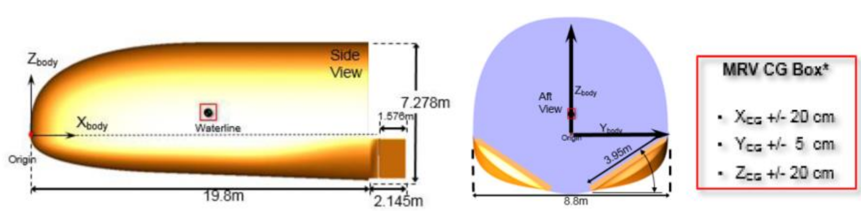

Figure 6. CG Box Definition.

Figure 2. Mid Lift to Drag (L/D) Mars Entry Vehicle (Ref. 2)

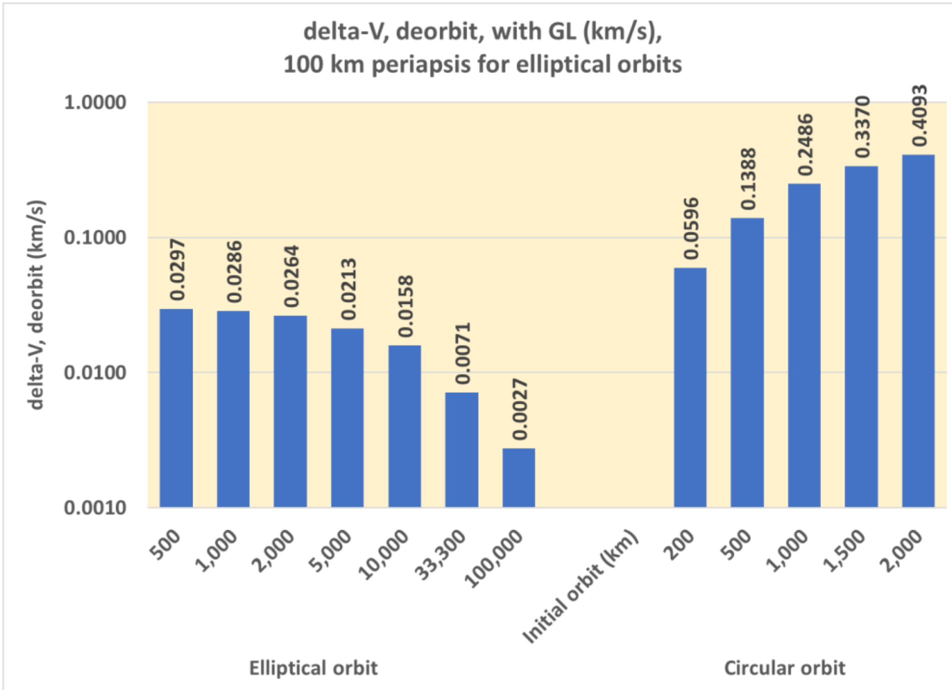

Figure 3. Deorbit delta-V for elliptical and circular Mars orbits

2.2 Deorbiting

The deorbit delta-V was computed for circular and elliptical Mars orbits. Many different human Mars Missions first enter an elliptical capture orbit. Such an elliptical orbit reduces the delta-V needed for the initial capture into Mars' orbit. Successive orbit transfer maneuvers may be completed to circularize the orbit.

For the deorbit from the elliptical orbit, the deorbit delta-V is delivered at the apoapsis of the elliptical orbit, slowing the lander into a new elliptical orbit that has a periapsis altitude of zero km.

From a circular orbit, the deorbit delta-V is the delta-V to place the lander on an elliptical transfer whose periapsis altitude is zero km.

2.3 Deceleration and Soft Landing

Once the lander has completed the deorbit maneuver, the lander will proceed toward the atmosphere. The atmosphere then slows the lander until it reaches its terminal velocity.

The soft landing delta-V was computed using the terminal velocity of the landing vehicle. The terminal velocity is calculated using this equation:

V, terminal = square root (Lander initial mass x g, Mars / (Area x Cd x density x 0.5))

Or:

$$V, terminal = \sqrt{\ }\left(\left(Lander\ initial\ mass\ x\ g, Mars\right) / \left(Area\ x\ Cd\ x\ density\ x\ 0.5\right)\right)$$

The deceleration delta-V (or V, terminal) values are provided in Figures 4 and 5. Figure 4 is for the frontal area of 40 m^2 and Figure 5 presents the calculations for an 80 M^2 frontal area. The low L/D lander design with 80 m^2 was used for the lander initial mass calculations. The 40 m^2 cases would represent a smaller lander, perhaps for one-way cargo only.

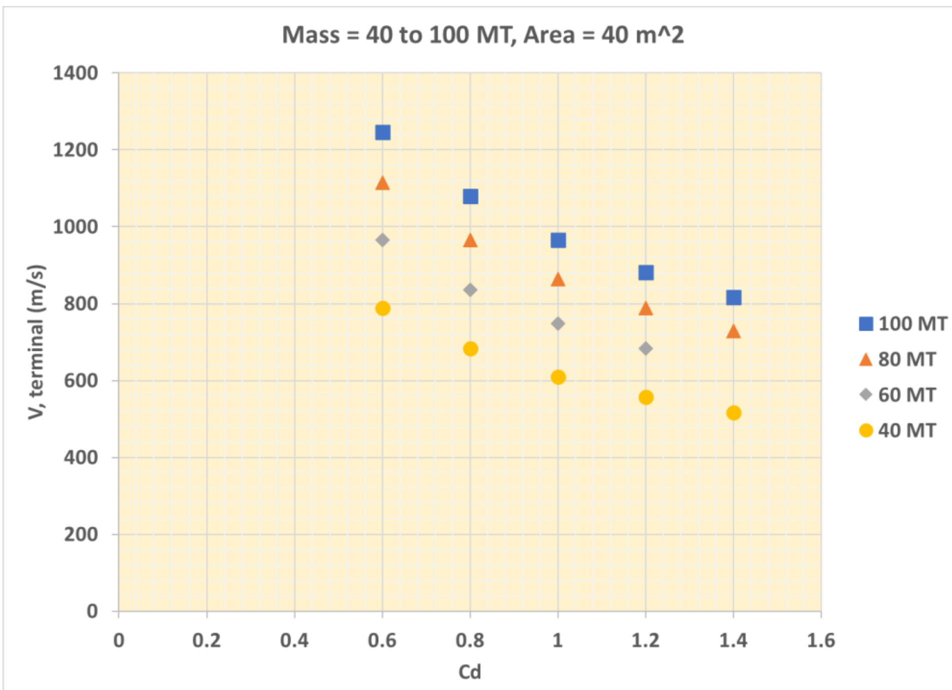

Figure 4 – Mars deceleration delta-V, area = 40 m^2

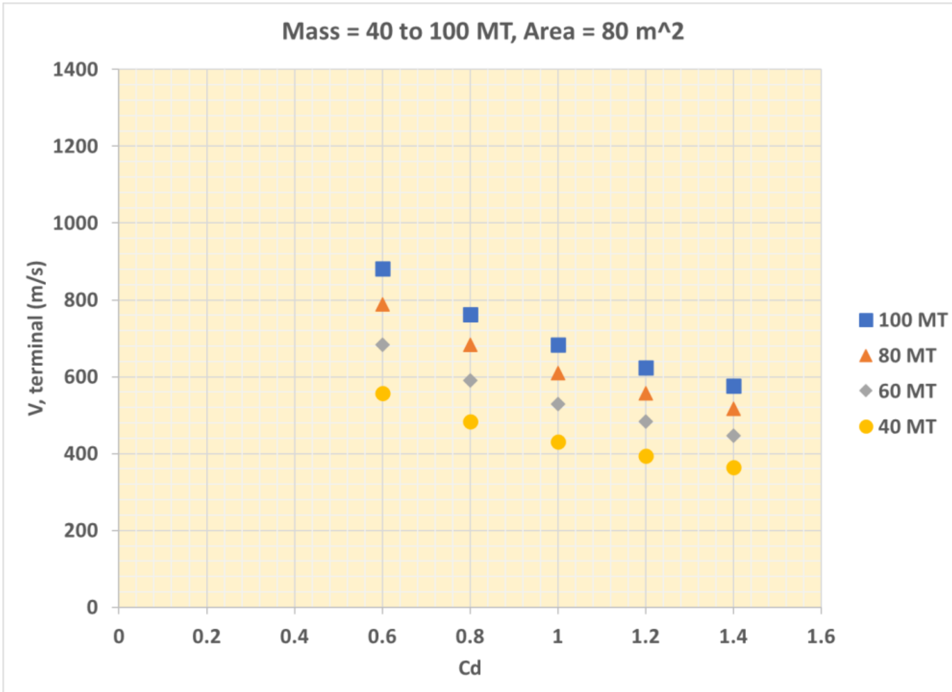

Figure 5 – Mars deceleration delta-V, area = 80 m^2

2.4 Hovering

After the lander has decelerated to zero velocity, the lander will hover to select the best landing site. The hover delta-V was completed using the firing time of the lander rocket engine. For the initial lander mass, the maximum hover thrust level is completed: the hovering thrust equals the initial weight of the lander. The mass flow for that hovering thrust level is multiplied by the firing time to compute the total hovering propellant mass; the total hovering propellant mass is then used to complete the hovering delta-V.

In Figure 6, the delta-V for hovering is shown to be somewhat independent of the rocket engine specific impulse (Isp). Tables 1 and 2 compares the hovering delta-V for three engine Isp values. For a 10 second hover time and an Isp of 460 seconds, the delta-V is 37.4 m/s. The hovering delta-V does not include any gravity losses.

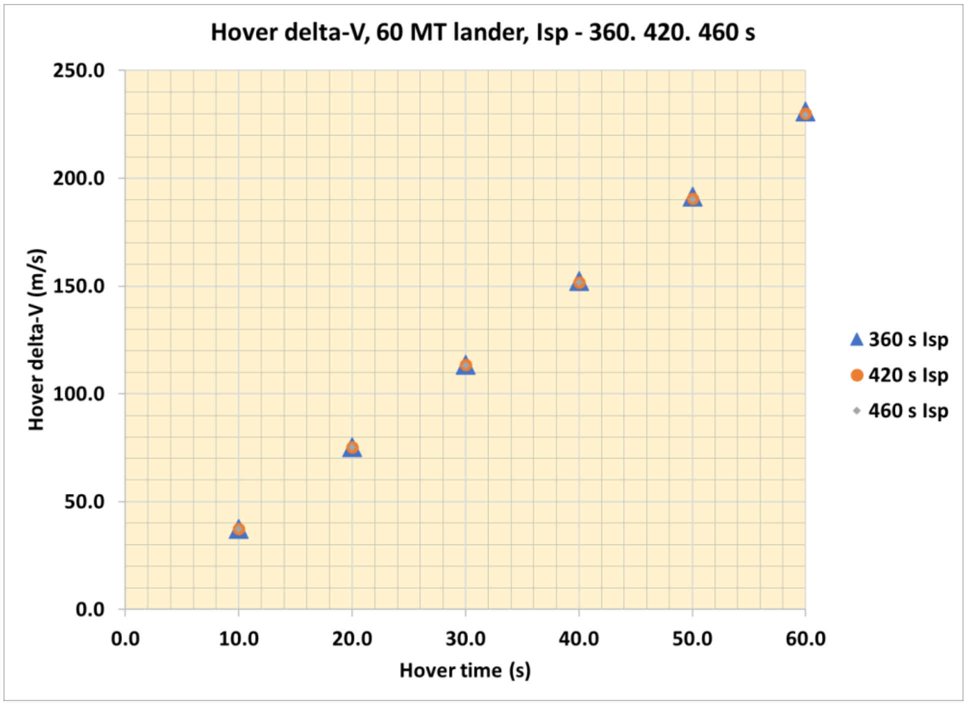

Figure 6. Hovering delta-V for 10 to 60 seconds: Isp values of 360, 420, and 470 seconds

mass, MT	60	60	60	60	60	60
	2,200	2,200	2,200	2,200	2,200	2,200
mass, lbm	132,000	132,000	132,000	132,000	132,000	132,000
g, Earth	9.81	9.81	9.81	9.81	9.81	9.81
Mars fractional g	0.38	0.38	0.38	0.38	0.38	0.38
g, Mars, m/s	3.7278	3.7278	3.7278	3.7278	3.7278	3.7278
F, lbf	50,160	50,160	50,160	50,160	50,160	50,160
Isp, s	460	420	360	460	420	360
m-dot, lbm/s	109.043	119.429	139.333	109.043	119.429	139.333
t, hover, s	10	10	10	60	60	60
Mp, hover, lbm	1,090.435	1,194.286	1,393.333	6,542.609	7,165.714	8,360.000
Mp, hover, MT	0.496	0.543	0.633	2.974	3.257	3.800
	59.504	59.457	59.367	57.026	56.743	56.200
delta-V, hover, m/s	37.433	37.448	37.476	229.401	229.968	231.065

Table 1. Hovering delta-V calculations

Hover delta-V (m/s)						
t, hover (s)	10.0	20.0	30.0	40.0	50.0	60.0
360 s Isp	37.5	75.4	113.6	152.4	191.5	231.1
420 s Isp	37.4	75.2	113.4	151.9	190.7	230.0
460 s Isp	37.4	75.2	113.2	151.6	190.3	229.4

Table 2. Hovering delta-V calculations summary: showing delta-V being insensitive to Isp

2.5 Ascent to Mars orbit

To compute the ascent delta-V to the final orbit, there are 2 calculations. The first is the ascent to the low Mars orbit was calculated. Once in the initial low circular orbit, the delta-V to reach the required circular orbit is computed. For the elliptical orbit, the transfer orbit to the final orbit is then calculated.

In Figure 7, the delta-V for the elliptical and circular orbits is presented. As an example, the delta-V to reach the 33,300 km apogee orbit was 5.7 km/s. Three engine firing are needed: two firings are used to reach the initial 100 km circular orbit and one added firing to enter the elliptical orbit.

For a 500 km circular orbit, the total delta-V was 4.4 km/s. There are 4 engine firing needed: two firings to enter the 100 km low circular orbit and two firings to enter the 500 km circular orbit.

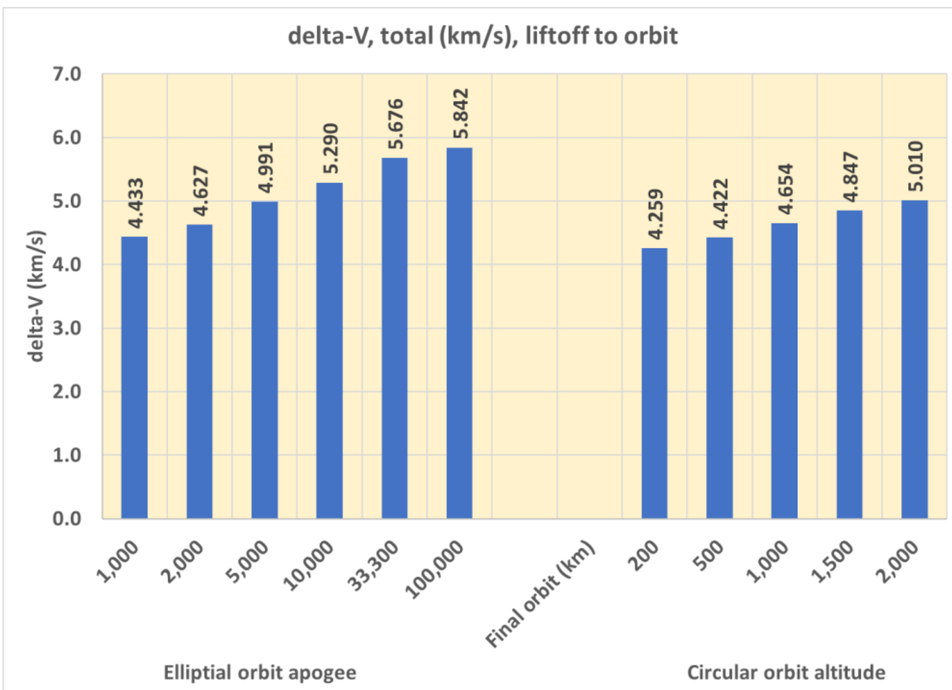

Figure 7. Ascent delta-V for elliptical and circular orbits

	Table I. Example delta-V summary		
Descent maneuvers:	delta-V (m/s)	Comment	Comments
Deorbit	138.8	Deorbit from 500 km, circular	Gravity loss = 20%
Deceleration	636.0	Initial mass = 60 MT, area = 80 m^2, Cd = 1.0	Gravity loss = 20%
Hover	38.0	Hover = 10 seconds	
Total	812.8		
Ascent maneuvers:	delta-V (m/s)	Comment	Comments
Ascent to LMO	4,200.0	Ascent to LMO, 100 km, circular	Gravity loss = 20%
Orbit transfer to final orbit	244.8	Transfer to 500 km, circular	Gravity loss = 20%
Total	4,444.8		
Total of ascent and descent	5,257.6		

Table 3. Lander delta-V summary for 500 km circular orbit

	Table I. Example delta-V summary		
Descent maneuvers:	delta-V (m/s)	Comment	Comments
Deorbit	0.00710	Deorbit from 33,300 km, elliptical	Gravity loss = 20%
Deceleration	636.00000	Initial mass = 60 MT, area = 80 m^2, Cd = 1.0	Gravity loss = 20%
Hover	38.00000	Hover = 10 seconds	
Total, descent	674.00710		
Ascent maneuvers:	delta-V (m/s)	Comment	Comments
Ascent to LMO	4,200.00000	Ascent to LMO, 100 km, circular	Gravity loss = 20%
Orbit transfer to final orbit	1,476.00000	Transfer to 33,300 km, elliptical	Gravity loss = 20%
Total, ascent	5,676.00000		
Total of ascent and descent	6,350.00710		

Table 4. Lander delta-V summary for 33,300 km orbit (24 hour orbit)

3.0 Mars landing vehicle sizing cases

Mars landing and ascent propulsion requirements often lead to high delta-V values. The delta-V requirements include the maneuvers from Tables 3 and 4. While the total descent delta-V is less than 1,000 m/s, the ascent delta-V to attain a 100 km low Mars orbit (LMO) is 4,200 m/s. The descent and ascent delta-V values include an additional 20% to address gravity losses during flight.

Mass scaling equations were developed for the Mars landers. The mass scaling was simplified based on historical data and analyses. For the two stage landers, the mass scaling equation was

Mdry = B x Mp

Where

Mdry = propulsion system dry mass, kg

B = propulsion dry mass fraction, kg / kg propellant, = 0.4

Mp = propellant mass, kg

For the single stage landers, the mass scaling equation structure was the same as the two-stage lander, however, the B factor is varied from 0.1 to 0.25. This B factor variation reflected the wide range of historical design analyses. The variation represents that varying aerodynamic designs and the varying structural mass estimates.

Two, single stage lander designs were assessed. The payload masses were 5 and 15 MT. The single stage vehicle is based on the concept proposed in Ref. 7. The initial masses of the single stage vehicles are shown in Figures 8 and 9. For the 15 MT round trip payload using a dry mass factor (B) of 0.2, the initial mass is 226 MT, as shown in Figure 8. This mass is substantially higher than the 105 MT mass estimated in Ref. 7; a B factor of 0.1 was used in that analysis. In the Ref. 7 concept, refueling of the sortie vehicle would be conducted from water either brought from earth or mined from the martian moons.

The 5 MT payload single stage sortie vehicle with a dry mass factor (B) of 0.2 has an initial mass of 76 MT, shown in Figure 9. This vehicle has a mass more akin to that proposed in Ref. 7.

Analyses of the martian moons predicted that the time for mining the needed propellant will be very long (Refs. 10, 11). Additional analyses of the in-situ resource utilization (ISRU) factories to support the refueling will be important future investigations (Ref. 12).

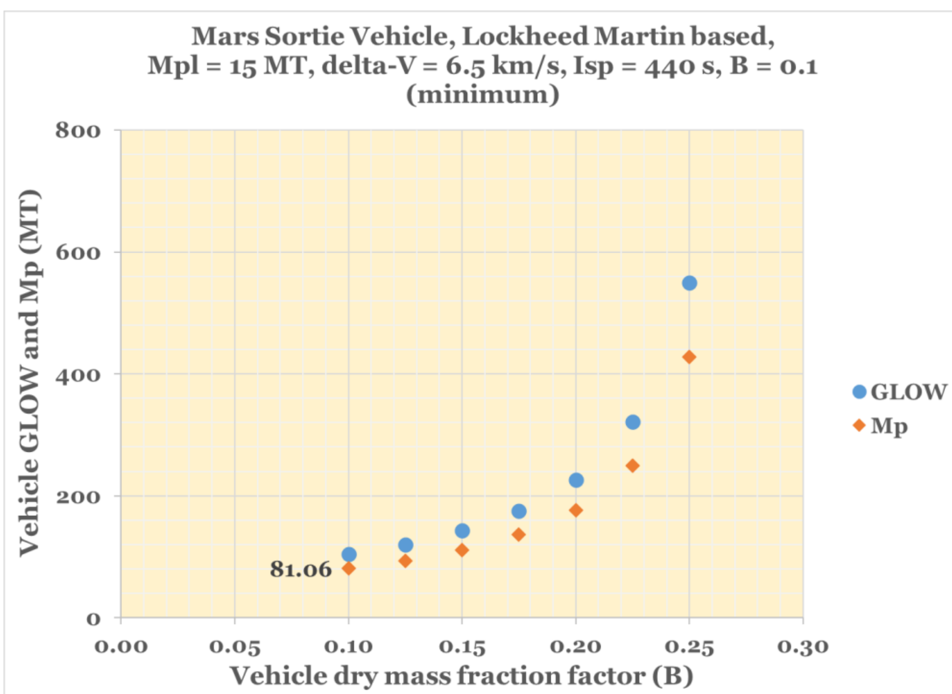

Figure 8. Single stage Mars lander: GLOW versus dry mass factor (B), 15 MT round trip payload

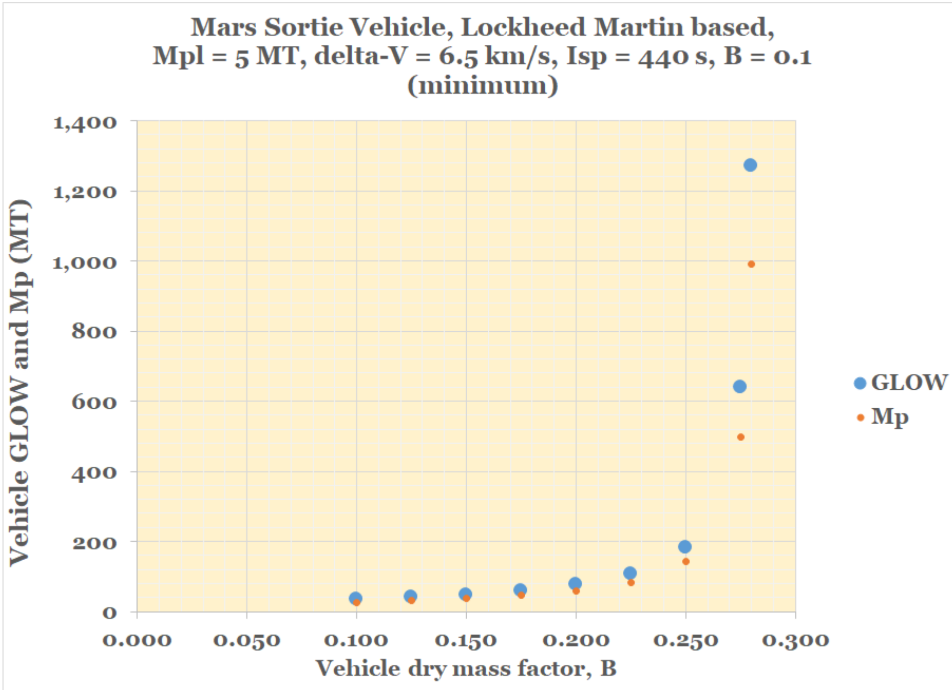

Figure 9. Single stage Mars lander: GLOW versus dry mass factor (B), 5 MT round trip payload

Table 5 provides a mass and performance summary for a two stage Mars landing vehicle. Each stage used an oxygen/hydrogen (O2/H2) chemical propulsion system and the stage masses reflect the delta-V values of Table 3. The round trip payload is mass is 5,100 kg; this mass represents accommodations for the human crew.

Four two-stage lander cases were assessed. The cases are summarized in table 5.

	Round trip payload (MT)	Payload left on surface (MT)	Engine Isp (s)	B factor	Initial mass (MT)
Case 1	5.1	0	460	0.4	59.375
Case 2	5.1	10	460	0.4	73.025
Case 3	5.1	25	460	0.4	93.500
Case 4	5.1	25	470	0.4	85.614

Table 5. Two stage lander designs: assessed cases

Case 1 shows the mass summary for the 5.1 MT crew only lander in Table 6. The lander uses a dry mass factor (B) of 0,4 for each stage. The Isp value for both stages is 460 seconds. The total delta V for the round trip mission is approximately 5.3 km/s. The lander initial mass if 59.4 MT.

The landers shown in Tables 7 and 8 show the influence of adding a landed payload of 10 and 25 MT, respectively. The lander initial mass for the 10 MT landed payload is 73.0 MT, an increase of 13.6 MT over the 59.4 MT Case 1 lander.

Parameter	Mars, ascent stage, round trip	Mars, descent stage, round trip
	O2/H2	O2/H2
Delta-V (m/s)	4,444.80	812.80
Isp (s)	460.00	460.00
G (m/s^2)	9.81	9.81
Mdry fraction	0.40	0.40
Entry capsule (kg)	5,100.00	
Adapter mass (kg)	510.00	
Adapter fraction	0.10	
Mp/l (kg)	5,610.00	45,673.71
e^x	2.68	1.20
Mp (kg)	28,616.93	9,786.69
Mdry (kg)	11,446.77	3,914.68
GLOW (kg)	45,673.71	59,375.07

Table 6. Two-stage lander with 5.1 MT round trip payload, crew only: Isp = 460 s

Parameter	Mars, ascent stage, round trip		Mars, descent stage, round trip
	O2/H2		O2/H2
Delta-V (m/s)	4,444.80		812.80
Isp (s)	460.00		460.00
G (m/s^2)	9.81		9.81
Mdry fraction	0.40		0.40
Entry capsule (kg)	5,100.00		
Adapter mass (kg)	510.00		
Adapter fraction	0.10	Adapter fraction	0.05
		Descent payload (kg)	10,000.00
Mp/l (kg)	5,610.00		56,173.71
e^x	2.68		1.20
Mp (kg)	28,616.93		12,036.57
Mdry (kg)	11,446.77		4,814.63
GLOW (kg)	45,673.71		73,024.90

Table 7. Two-stage lander with 5.1 MT round trip payload, 10 MT down payload: Isp = 460 s

Parameter	Mars, ascent stage, round trip		Mars, descent stage, round trip
	O2/H2		O2/H2
Delta-V (m/s)	4,444.80		812.80
Isp (s)	460.00		460.00
G (m/s^2)	9.81		9.81
Mdry fraction	0.40		0.40
Entry capsule (kg)	5,100.00		
Adapter mass (kg)	510.00		
Adapter fraction	0.10	Adapter fraction	0.05
		Descent payload (kg)	25,000.00
Mp/l (kg)	5,610.00		71,923.71
e^x	2.68		1.20
Mp (kg)	28,616.93		15,411.38
Mdry (kg)	11,446.77		6,164.55
GLOW (kg)	45,673.71		93,499.64

Table 8. Two-stage lander with 5.1 MT round trip payload, 25 MT down payload: Isp = 460 s

Parameter	Mars, ascent stage, round trip		Mars, descent stage, round trip
	O2/H2		O2/H2
Delta-V (m/s)	4,444.80		812.80
Isp (s)	470.00		470.00
G (m/s^2)	9.81		9.81
Mdry fraction	0.40		0.40
Entry capsule (kg)	5,100.00		
Adapter mass (kg)	255.00		
Adapter fraction	0.05	Adapter fraction	0.05
		Descent payload (kg)	25,000.00
Mp/l (kg)	5,355.00		66,242.45
e^x	2.62		1.19
Mp (kg)	24,741.04		13,837.13
Mdry (kg)	9,896.42		5,534.85
GLOW (kg)	39,992.45		85,614.44

Table 9. Two-stage lander with 5.1 MT round trip payload, 25 MT down payload: Isp = 470 s

The Case 3 lander has an initial mass of 93.5 MT and has a landed payload of 25 MT. The initial mass increased by 20.5 MT over the Case 2 lander. In Case 4, the landed payload is 25 MT and the Isp has been increased from 460 to 470 seconds. the initial mass is 85.6 MT, saving 8 MT over the 460 second Isp case.

In these analyses, the lander delta-V has remained constant for all cases. In general, due to the vehicle initial mass, each case has a different delta-V. The difference is driven by the difference terminal velocities of the deceleration phase. More refined analyses would show that the higher initial mass cases would have higher delta-V values and lead to additional initial mass increases. Therefore, the influence of Isp increases will be even more important as higher and higher payloads are needed for the Mars architectures.

4.0 Conclusions

The Mars lander systems using chemical propulsion were analyzed. The delta-V values for the descent and ascent were computed for a wide range of circular and elliptical orbits were computed. These analyses provide a design toolbox to assess a wide variety of mars landing architectures.

In general, two stage landers allow large payloads to be delivered with masses between 60 and 100 MT. The dry mass fraction of 0.4 may allow for more mass growth and a more flexible design. Using 2 stages makes the stage more forgiving of design mass growth if mass control is a potential issue.

The single stage landers will require more aerodynamic maneuvering (as with the Ref. 7 design), making the thermal protection design more complex than the two-stage designs. Potentially, the single stage landers allow for a more sustainable lander architecture when using oxygen / hydrogen propulsion rocket engines refueling with martian water ice. The first Mars landers will likely be the more conservative two-stage designs.

While ISRU was not assessed in detail, past analyses have shown that mining of the martian moons will be a potentially difficult process (Ref. 10, Palaszewski). More analyses of the ISRU options on the martian surface are continuing and are a more likely option for any sustainable Mars missions (Ref. 12).

References:

1) G. R. Woodcock, "AN INITIAL CONCEPT OF A MANNED MARS EXCURSION VEHICLE FOR A TENOUS MARS ATMOSPHERE," NASA MSFC, Advanced Systems Office, NASA TECHNICAL MEMORANDUM, TM X-53475, June 7, 1966.
2) Johnson, B., et al., Entry, Descent, and Landing Performance for a Mid-Lift-to-Drag Ratio Vehicle at Mars, NASA Johnson Space Center, JSC-E-DAA-TN51349, 2018 American Astronautical Society Guidance and Control Conference February 2018.
3) *Report of the 90-Day Study on Human Exploration of the Moon and Mars" (PDF). NASA. November 1989.*, NASA Headquarters, 1989. history.hq.nasa.gov

4) Palaszewski, B., Metallized Propellants for the Human Exploration of Mars, NASA TP 1990-3062, November 1990.
5) Woodcock, Gordon R., “Space transfer concepts and analyses for exploration missions, phase 4,” Boeing *Defense and Space Group Huntsville, AL,* Contractor Report (CR) D615-10070, NASA-CR-193849, September 1, 1993.
6) Drake, Bret G., “Human Exploration of Mars Design Reference Architecture 5.0,” *NASA Johnson Space Center Houston, TX,* JSC-CN-35516, NASA/SP-2009-566-ADD2, January 1, 2010
7) Timothy Cichan, Sean O’Dell, Danielle Richey, Stephen A. Bailey, Adam Burch, “MARS BASE CAMP UPDATES AND NEW CONCEPTS,” Lockheed Martin Corporation. IAC-17,A5,2,7,x40817, 68th International Astronautical Congress (IAC), Adelaide, Australia, 25-29 September 2017.
8) Roger R. Bate, Donald D. Mueller, Jerry E. White, “Fundamentals of Astrodynamics,” Dover Books on Aeronautical Engineering, Jan 1971.
9) Edelbaum, T. N., “Propulsion Requirements for Controllable Satellites,” ARS Journal, Vol. 31, Aug. 1961, pp. 1079–1089.
10) Palaszewski, B., Martian Moons and Space Transportation Using Chemical and Electric Propulsion Options Book title: **Solar System Planets and Exoplanets,** 06-2021, https://www.intechopen.com/books/solar-system-planets-and-exoplanets
11) “First International Conference on the Exploration of Phobos and Deimos,” LPI contribution number 1377, held at NASA Ames Research Center, November 5-7, 2007.
12) Sanders, G., et al. Current NASA Plans for *Mars* In Situ Resource Utilization, JSC-E-DAA-TN52598, February 20, 2018,